FLEXURAL BEHAVIOR OF LIGHTWEIGHT AGGREGATE CONCRETE FILLED STEEL TUBE

Fu Zhongqiu, Ji Bohai*, Maeno Hirofumi, Eizien A. and Chen Jiashu

College of Civil and Transportation Engineering, Hohai University, Nanjing 210098, China
**(Corresponding author: E-mail: hhbhji@163.com)*

Received: 28 September 2012; Revised: 24 March 2013; Accepted: 18 October 2013

ABSTRACT: To study the flexural behaviour of lightweight aggregate concrete filled steel tubes (LACFST), 21 LACFST specimens and 8 steel tubes without filling concrete were tested under pure bending load. The parameters considered are: steel tube diameter and thickness, lightweight aggregate concrete (LAC) strength and shear span ratio. According to the test results, the failure mode, deflection and failure process were studied and their influence on the flexural behaviour of LACFST was analyzed. Several codes were used to calculate the stiffness and moment capacity. Based on the mechanical equilibrium and combined strength, two methods were provided to calculate the moment capacity in this paper. The calculated results were verified with the test ones. The constitutive model of confined LAC in compressive region was also proposed and used in the FEM to analyze the flexural behaviour of LACFST. This study showed the strain distribution agreed with the Bernoulli-Euler's theory. The deflection along the length distributed as half sine wave curve during the test. The moment capacity of LACFST increased as the steel ratio and LAC strength increased. But the shear span ratio had almost no influence on the flexural behaviour of LACFST. The comparison between the calculation and the test showed the results of AIJ (1997) for stiffness and DL/T5085 for moment capacity fitted with the test ones well. But the results using the two proposed methods had a better accuracy to calculate the moment capacity. The FEM analysis showed the constitutive model of confined LAC in compressive region was also proved having a good accuracy.

Keywords: Lightweight aggregate concrete filled steel tube, flexural behaviour, stiffness, moment capacity, calculation method

1. INTRODUCTION

Recently concrete filled steel tube (CFST) has wide applications in structures because of its high bearing capacity, lightweight, small cross section, good seismic performance and so on [1-4]. Under compressive loading, steel casing in CFST provides potential confinement to the concrete core which boosts the capacity and ductility of the concrete. Also concrete core can delay steel tube local buckling appearance. Therefore, CFST is always used as compression members. But because of the high bearing capacity and small cross-sectional area, it is application as a beam structure has advantages too.

Many researchers have focused their studies on the behavior of CFST at the practical application [5-7]. Therefore, a flexural performance of CFST needs to be studied more deep theoretically [8-10]. In fact, CFST has already been used as flexural member of bridges, such as the composite beam of Shinkansen bridge in Japan [11]. In China, there are 5 CFST space truss beam bridges already which are Zidong Bridge in Guangdong, Xiangjiaba Bridge in Hubei, Wanzhou Bridge in Chongqing, Wan`ang Bridge in Chongqing, Ganhaizi Bridge in Sichuan.

According to the beam, especially the large span ones, their self-weight has a significant impact on their structural behavior. Thus, as the lightweight aggregate concrete has lighter weight than the normal concrete it may replace the second one to fill the steel tubes. Previous researches [12-13] show that LACFST has excellent mechanical performance which is similar to that of CFST. Also, they confirmed that LACFST can be used in structures instead of CFST. In addition, if LACFST applied in beams, the height of the beam section and the cost of the basis will obviously reduced.

In 2003, Assi IM studied 34 square and rectangular steel tubes (1000mm length) filled with foamed and lightweight aggregate concrete experimentally to evaluate the ultimate moment of these beams [14]. But till now, there is a few researches concern the flexural performance of LACFST beams. Although, there are some flexural performance conclusions about normal CFST, it is not decided yet whether these conclusions are applicable to LACFST or not till now. Thus, there is a need for more studies in this concern. Based on the previous studies carried by the authors [15-16] on the compressive performance of LACFST, the behavior of circular LACFST under pure bending was studied.

2. EXPERIMENTAL INVESTIGATIONS

2.1 Material

The coarse aggregate of lightweight aggregate concrete is haydite. The bulk density is 814 kg/m^3, the cylindrical compressive strength is 8.5MPa, and the ratio of water absorption ratio is 6% an hour. Ordinary Portland cement was used for the concrete. According to the relevant Chinese standards, compression tests were carried out on a number of standard cubes ([150×150×150] mm) to determine the concrete grade and prisms [150×150×300] mm in order to determine the compressive strength (f_{ck}) and elastic modulus (E_c) of the unconfined concrete. The cubes and prisms were cured at room temperature. The concrete mix proportion and mechanical properties are given in Table 1 and Table 2 respectively.

Table 1. Mixture Mass per Cubic Meter LAC Concrete (kg)

Item	Cement	Haydite	Sand	Water	Mineral powder	Water reducer
Mix 1	460	670	650	170	0	0
Mix 2	450	650	650	125	50	3

Table 2. Mechanical Properties of LAC Concrete

Item	Cubic strength 28d f_{cu} (MPa)	Cubic strength 105d f_{cu} (MPa)	Prism strength 105d f_{ck} (MPa)	Elastic Modulus E_c (GPa)	Bulk density (kg/m^3)
Mix 1	44.8	49.9	31.3	24.0	1810
Mix 2	53.6	59.2	41.2	26.8	1910

Straight welded steel tube Q235 was used in the test. A group of three standard specimens tested to determine the tensile strength of the steel where the thickness of each section of steel tube made into the interception of the standard specimen. The test method followed the regulations of Chinese standard "Metallic materials at ambient temperature tensile test method" (GB/T228-2002) (2002). The data was collected by TS3890 pseudo-dynamic strain instrument during the test process. The stress and strain relationship of specimen is shown in Figure 1. The Yield strength is 298.5 MPa and 274.7MPa for the steel with 2.5mm thickness and 3.8mm thickness respectively. The yield strain can be taken as $\varepsilon = 2000\times10^{-6}$ from Figure 1.

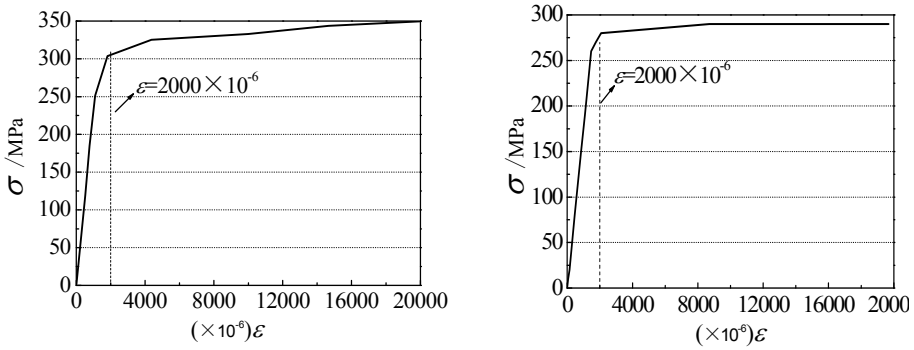

(a) t=2.5mm (b) t=3.8mm

Figure 1. Stress versus Strain Curve of Steel

2.2 Specimen

In this study, 21 LACFST specimens and 8 steel tube specimens without filling concrete were tested. Two types of steel tube used with diameters of 114mm and 165mm. The total length L of steel tube was 1400mm and 1700mm with effective span L_o =1200mm and 1500mm respectively. The two ends of the steel tube were flatted then, before concrete pouring, a circular plate with 8mm thickness welded on one end of each tube. During concrete pouring, the angle between the steel tube and the ground was larger than 70°. Then, a concrete shaking table used to vibrate it and to ensure its density. Two weeks later, surface hollows due to shrinkage filled up with grout to confirm the specimen side smoothness. To observe the slip between the steel tube and LAC, two identical circular plates welded on both ends of some of the test specimens, while the rest of the specimens welded on one end only. The specimens cured by natural conditions. The details of the test specimens are shown in Table 3.

Table 3. Details of the Test Specimens

Specimens	Pipe size (mm)			L_o (mm)	L_a (mm)	λ	α	f_y (MPa)	f_{ck} (MPa)	M_u (kN • m)
	D	t	L							
CS114-2.5-30-A	114	2.5	1400	1200	300	2.6				11.47
CS114-2.5-30-B	114	2.5	1400	1200	300	2.6	0.09	298.5	31.3	11.75
CS114-2.5-30-C	114	2.5	1400	1200	300	2.6				12.02
CS114-2.5-50-A	114	2.5	1400	1200	300	2.6				13.17
CS114-2.5-50-B	114	2.5	1400	1200	300	2.6	0.09	298.5	41.2	11.94
CS114-2.5-50-C	114	2.5	1400	1200	300	2.6				12.3
CS114-3.8-30-A	114	3.8	1400	1200	300	2.6				14.72
CS114-3.8-30-B	114	3.8	1400	1200	300	2.6	0.14	274.7	31.3	15.88
CS114-3.8-30-C	114	3.8	1400	1200	300	2.6				15.08
CS114-3.8-50-A	114	3.8	1400	1200	300	2.6				17.56
CS114-3.8-50-B	114	3.8	1400	1200	300	2.6	0.14	274.7	41.2	16.13
CS114-3.8-50-C	114	3.8	1400	1200	300	2.6				16.56
CS165-2.5-30-A	165	2.5	1400	1200	300	1.8				20.72
CS165-2.5-30-B	165	2.5	1400	1200	400	2.4	0.06	298.5	31.3	22.96
CS165-2.5-30-C	165	2.5	1700	1500	500	3.0				21.48
CS165-3.8-30-A	165	3.8	1400	1200	300	1.8				37.81

CS165-3.8-30-B	165	3.8	1400	1200	400	2.4	0.09	274.7	31.3	36.93
CS165-3.8-30-C	165	3.8	1700	1500	500	3.0				37.9
CS165-3.8-50-A	165	3.8	1400	1200	300	1.8				37.8
CS165-3.8-50-B	165	3.8	1400	1200	400	2.4	0.09	274.7	41.2	40.08
CS165-3.8-50-C	165	3.8	1700	1500	500	3.0				38.7
ST114-2.5-A	114	2.5	1400	1200	300			298.5		9.73
ST114-2.5-B	114	2.5	1400	1200	300					9.78
ST114-3.8-A	114	2.5	1400	1200	300			274.7		12.57
ST114-3.8-B	114	3.8	1400	1200	300					12.48
ST165-2.5-A	165	2.5	1400	1200	300			298.5		16.38
ST165-2.5-B	165	2.5	1400	1200	300					16.00
ST165-3.8-A	165	3.8	1400	1200	300			274.7		31.45
ST168-3.8-B	165	38	1400	1200	300					30.64

Note: 1. D is the external diameter, t is the thickness, L, L_o, L_a stand for the length in Figure 2;
2. f_y is the yield strength of steel, f_{ck} is the prism strength at 105d;
3. α is steel ratio, $\alpha=A_s/A_c$, here A_s is the area of steel, A_c is the area of concrete;
4. λ is the shear span ratio, $\lambda=L_a/D$;
5. M_u is test ultimate moment corresponding to the load when the steel strain is 0.01.

2.3 Test Instruments and Procedure

This experiment performed in the structural engineering laboratory of Hohai University. The details of the test instruments sketched in Figure 2. The load applied on a rigid beam by a hydraulic jack and measured by a pressure sensor. A four-point bending rig used to apply the moment (see Figure 2a). 4 groups and 8 groups of strain gauges set at midspan of each specimen and spread eventually through the beam diameter (114mm and 165mm) respectively. Each group had a longitudinal strain gauge and a hoop strain gauge. There were 5 displacement transducers set to measure the deflection along the span, 3 of them set at one–quarter point and 2 of them set at the supports positions.

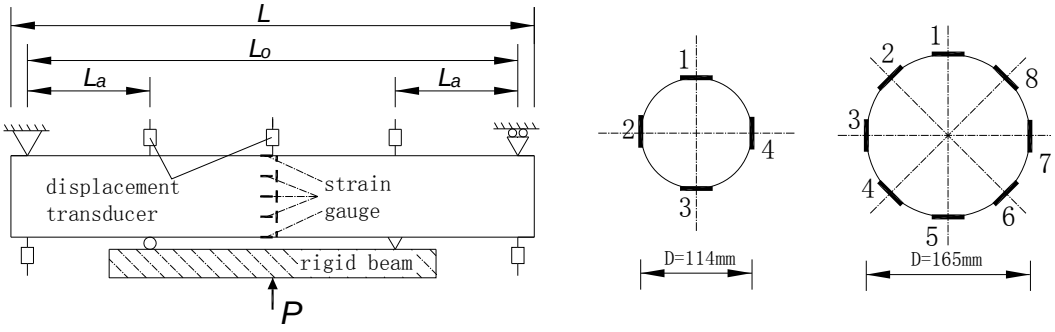

(a) Loading installations (b) Distribution of strain gauges

Figure 2. Loading and Measurement System

The specimens loaded at rate of 1/10 and 1/15 of the predicted ultimate load in the elastic phase and in the yielding phase respectively. Each load maintained about 2-3 minutes to enable the full deformation development. When approaching the predicted ultimate load, the load added slowly. All the gauges used in this experiment connected to a computer data acquisition system to record their values in the whole test phases (See Figure 3).

Figure 3. General View of the Test Setup

Figure 4. Specimen Failure Modes

3. EXPERIMENTAL RESULTS

3.1 Failure Mode

Figure 4 shows typical failure modes of LACFST beam. Although, most specimens failed without local buckling but a few of the specimens show unobvious local bucking at the rigid beam supports due to stress concentration caused by supports. Specimens welded on one end only show no slip between steel tube and LAC core. The cracked concrete took the shape of the deformed steel section. Besides, the cracks penetrated the whole section from tension area to compression area and spread evenly as was noticed after removing the steel wall as can be seen in Figure 4. This proved the section acted as a composite one, and the concrete confined by the steel tube. For the steel tube without filling, all specimens failed due to local buckling at the supports locations and mid-span.

3.2 Deflection of Specimen

Figure 5 shows a typically measured bending moment versus deflection curves of a group of specimens. From these curves noticed the defection increased slowly as the moment increased before the steel tube reach to the yield strain where, it is almost a straight line. After the steel tube yielding, the deflection increased rapidly. Moreover, all the curves showed no downward tendency when the test was stopped.

Figure 6 shows deflection curve along one of a typical tested specimen length under flexure. From this figure it is observed the curves are not symmetrical at the beginning of the test because of the discontinuity of materials. As the load increased, specimen deflection increased and distributed symmetrically due to stress redistribution between the concrete core and steel tube. Also it seemed the deflection curves coincided with half sine wave curves. And this had been improved in Figure 7 which showed the moment versus curvature curves of some specimens.

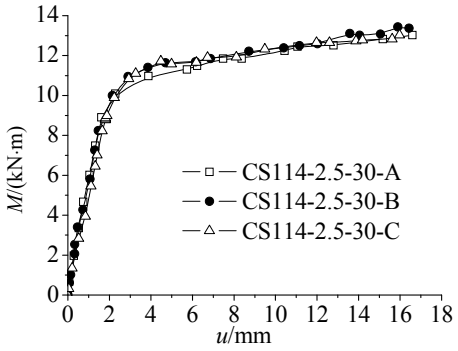

Figure 5. Moment Versus Deflection Curves

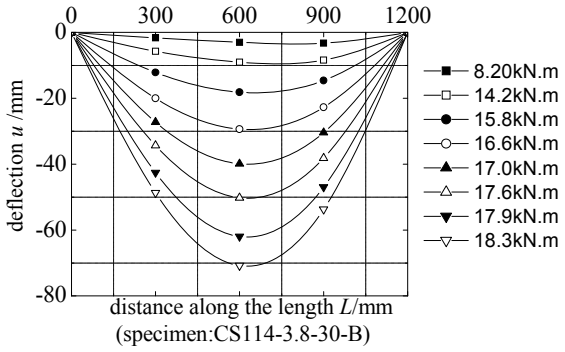

Figure 6. Deflection Distribution along the Length

For the flexural member, the curvature can be calculated with deflection and moment. And if the equation of deflection curve is known, it also can be calculated with the strain. Figure 7 displays the curves calculated by the two methods mentioned above. All the deflection and strain data were gained from the test. One of the curves was calculated by strain which was supposed that the deflection distributed as half sine wave curves. From the figures, it is possible to notice the clear convergence between the curves. So, it can be stated the deflection curve along the specimen length coincide with a half sine wave curve.

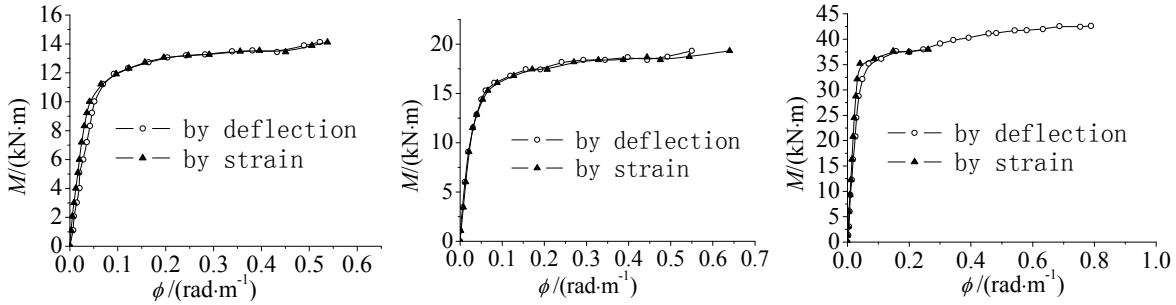

(a) CS114-2.5-50-A (c) CS114-3.8-50-A (e) CS165-3.8-30-B

Figure 7. Moment Versus Curvature Curves

3.3 Failure Process

Figure 8 shows the typical curves of moment versus steel longitudinal strain at the tension zone. All the curves of strain and deflection show there has no downward phase. So, the moment corresponding to the maximum fiber strain of 0.01 was defined as the moment capacity (M_u) of the specimen in this paper (refer to Figure 8) where its values listed in Table 3.

Figure 9 shows steel tube strain. At the beginning of the test, the axis of symmetry considered as the neutral axis of the section. Accordingly, strain 3 had almost no value before the tension side strain (strain 1) reach to yield strain (Strain numbers refer to the positions sketched in Figure 2(b)). All strains increased slowly in accordance to the moment increasing. After yield strain of tension side was reached, all strains increased rapidly. The neutral axis of the section moved, and the symmetry axis positioned in the original tensile zone thus, strain 3 increased as a tension strain.

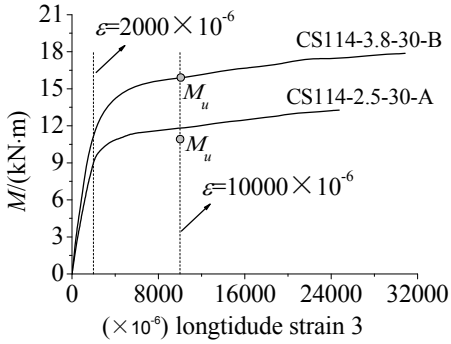

Figure 8. Demonstration of Moment Capacity

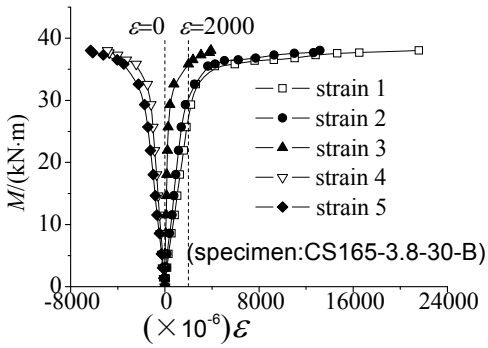

Figure 9. Longitudinal Strain of Steel Tube

Figure 10 describes the distribution curves of the longitudinal strains along the beam height. From the Figure it is noticed the section deformation of specimen's agree with the Bernoulli-Euler's theory at various loading stages. Neutral axis movement pointed out by the change of intersection point between connection line and symmetry axis.

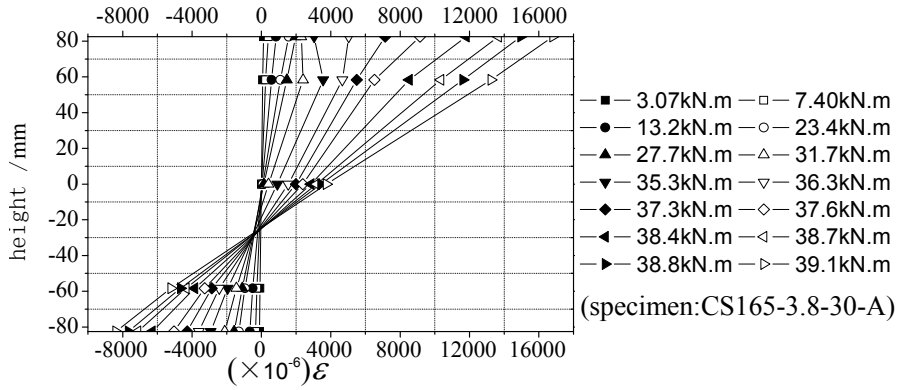

Figure 10. Distribution Curves of the Longitudinal Strain along the Beam Height

4. BEARING CAPACITY ANALYSIS

4.1 Influencing Factor

Figure 11(a) presents the moment - curvature curves of a specimen with different steel ratios. From the figure, it can be seen the initial stiffness of the specimen and the moment capacity increased as the steel ratio enlarged. In this test, specimens with t=3.8mm showed almost 30% moment capacity higher than the ones with t=2.5mm. As the steel has a higher bearing capacity; higher steel ratio will lead to more effective restrain to the concrete core. So, the higher steel ratio is the larger moment capacity and initial stiffness obtained.

From Figure 11(b) it is observed that specimen with higher LAC strength has a larger moment capacity. But, as it is known the moment mainly resisted by the steel tube, therefore; moment capacity increment was unobvious in compare with LAC strength improvement. Figure 11(c) shows the flexural behavior of LACFST and steel tube without concrete filling. From the figure it can be stated that LACFST has a better ductility and bearing capacity than the steel tube without concrete filling. Also, it can be concluded that filling steel tube with LAC can improve its flexural behavior well.

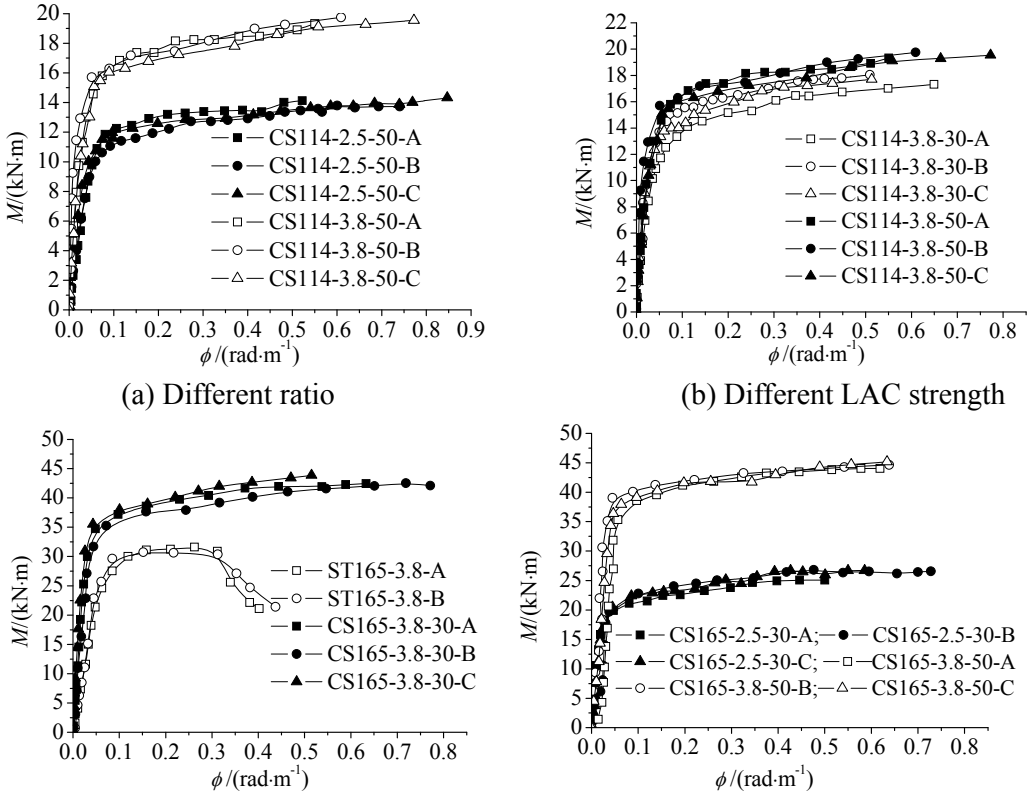

(a) Different ratio (b) Different LAC strength

(c) Comparison with steel tube (d) Different shear span ratio

Figure 11. Moment Versus Curvature Curves with Different Influencing Factor

Figure 11(d) displays the moment-curvature curves of specimens with different shear span ratio. From the figure it is possible to say the shear span ratio has almost no influence on the flexural behavior of LACFST.

4.2 Stiffness Calculation from the Codes

The stiffness of LACFST is a contribution of steel tube and LAC and not only the superposition of the two materials. When the specimen was flexural, the concrete would crack. The concrete could not provide enough stiffness to the composite beam and concrete core contribution to stiffness was reduced. A comparison between calculation formulas from different design codes carried out to study the stiffness of CFST, including AIJ (1997) [17], BS 5400 (1979) [18], EC4(1994) [19], AISC-LRFD (1999)[20] and DBJ13-15(2003)[21]. It was found that all the formulas can be described by expression (1).

$$K = E_s I_s + mE_c I_c \tag{1}$$

where E_s and E_c are the elastic modulus of steel and concrete; I_s and I_c are the moment of inertia of steel and concrete; m is concrete contribution reduction factor.

In different codes, E_s, E_c are defined different ways and determined from the constituent's materials. The reduction coefficient m takes various values in the different design codes as following: m=0.2 in AIJ (1997); m=1 in BS5400 (1979); m=0.26 in EC4 (1994); m=0.8 in AISC-LRFD (1999) and DBJ13-15(2003).

Table 4 Calculation and Test Results of Stiffness

Specimen	Test value		AIJ (1997)		BS5400 (1979)		EC4 (1994)		AISC-LRFD (1999)		DBJ13-51 (2003)	
	$K_{0.2}$	$K_{0.6}$	$\frac{K^C}{K_{0.2}}$	$\frac{K^C}{K_{0.6}}$	$\frac{K^C}{K_{0.2}}$	$\frac{K^C}{K_{0.6}}$	$\frac{K^C}{K_{0.2}}$	$\frac{K^C}{K_{0.6}}$	$\frac{K^C}{K_{0.2}}$	$\frac{K^C}{K_{0.6}}$	$\frac{K^C}{K_{0.2}}$	$\frac{K^C}{K_{0.6}}$
CS114-2.5-30	318.1	268.5	0.98	1.16	1.17	1.39	1.28	1.51	1.26	1.49	1.22	1.45
CS114-2.5-50	309.8	261.1	1.04	1.23	1.39	1.64	1.36	1.62	1.40	1.66	1.29	1.53
CS114-3.8-30	433.3	335.8	1.02	1.31	1.15	1.48	1.21	1.57	1.19	1.53	1.18	1.52
CS114-3.8-50	414.0	347.6	1.08	1.29	1.32	1.57	1.31	1.56	1.32	1.57	1.26	1.50
CS165-2.5-30	960.3	875.6	1.05	1.16	1.35	1.48	1.51	1.66	1.49	1.64	1.42	1.56
CS165-3.8-30	1313.0	1157.6	1.09	1.23	1.29	1.46	1.40	1.58	1.37	1.56	1.34	1.52
CS165-3.8-50	1292.1	1174.3	1.13	1.25	1.50	1.65	1.47	1.62	1.51	1.66	1.40	1.54
MEAN			1.06	1.23	1.31	1.53	1.36	1.59	1.36	1.59	1.30	1.52
STDEV			0.046	0.053	0.113	0.091	0.099	0.045	0.110	0.063	0.085	0.034

Different moments gained from the test due to the different stiffness. So, two stiffness values adopted to check the calculation results. The stiffness corresponding to $0.2M_u$ and $0.6M_u$ were defined as initial stiffness ($K_{0.2}$) and serviceability-level stiffness ($K_{0.6}$) respectively. Table 4 lists a comparison between the calculation and test results where, the test values are the average ones, and K^C is the value calculated by the codes.

From Table 4, AIJ code gave the best precision among the other codes compared in this paper. A mean value = 1.06 and a standard deviation (STDEV) = 0.046 for $K_{0.2}$ gained by AIJ code, while the other codes gave mean values with almost 30% more than the test results. For $K_{0.6}$, although AIJ gave a mean value =1.23 and STDEV = 0.053 which is not perfect result, the other codes gave mean values with 50% more the test results. So, it is possible to judge that AIJ code is the best predictor for LACFST beam stiffness and can be used to calculate it. Referring to Han Linhai [6], it can be decided the calculation results of LACFST are similar to those of normal concrete (CFST). Therefore, a value equal to 0.2 adopted for m in expression (1). And AIJ code is also suggested to calculate stiffness of LACFST.

4.3 Moment Capacity Calculation of Codes

Several expressions in different design codes for normal CFST used to calculate the moment capacity of the specimens. These expressions may be described as follows:
For AIJ (1997) [17]

$$M_u = Zf_y = \frac{D^3 - (D-2t)^3}{6} f_y \tag{2}$$

where f_y is the yield strength of steel; D is the diameter ; t is the thickness of steel tube.
For AISC-LRFD(1999)[20]

$$M_u = \phi_b Z f_y = \phi_b \frac{D^3 - (D-2t)^3}{6} f_y \tag{3}$$

where φ_b=0.9, the other parameters have similar definitions as it is described in Eq. 3.

For EC4 (1994) [19]

$$M_u = W_{pa} f_y / \gamma_s + \frac{1}{2} W_{pc} f_c^{'} / \gamma_c - W_{pan} f_y / \gamma_s - \frac{1}{2} W_{pcn} f_c^{'} / \gamma_c \tag{4}$$

$$W_{pc} = (D-2t)^3 / 4 - 2r^3 / 3 - r^2 (4-\pi)(0.5D - t - r) \tag{5}$$

$$W_{pa} = D^3 / 4 - 2(r+t)^3 / 3 - (r+t)^2 (4-\pi)(0.5D - t - r) - W_{pc} \tag{6}$$

$$W_{pcn} = (D-2t) h_n^2 \tag{7}$$

$$W_{pan} = D h_n^2 - W_{pcn} \tag{8}$$

$$hn = \frac{A_c f_c^{'} / \gamma_c}{2D f_c^{'} / \gamma_c + 4t(2 f_y / \gamma_s - f_c^{'} / \gamma_c)} \tag{9}$$

where γ_c=1.5; γ_s=1.1; f_c' is the cylindrical compressive strength of concrete; r is the internal radius; A_c is the area of concrete; the other parameters have similar definitions as description in Eq. 3.

For DLT5085 (1999) [22]

$$M_u = \gamma_m W_{sc} f_{sc} \tag{10}$$

$$\gamma_m = -0.4047\xi + 1.7629\sqrt{\xi} \tag{11}$$

$$f_{sc} = (1.212 + B_1 \xi + C_1 \xi^2) f_{ck} \tag{12}$$

$$B_1 = 0.1759 f_y / 235 + 0.974 \tag{13}$$

$$C_1 = -0.1038 f_{ck} / 20 + 0.0309 \tag{14}$$

where $\xi = A_s f_y / (A_c f_{ck})$; $W_{sc} = \pi D^4 / 32$; f_{ck} is the concrete strength; A_s and A_c is the area of steel and concrete respectively.

For DBJ13-51(2003) [21]

$$M_u = \gamma_m W_{sc} f_{sc} \tag{15}$$

$$\gamma_m = 1.1 + 0.48 \ln(\xi + 0.1) \tag{16}$$

$$f_{sc} = (1.14 + 1.02\xi) f_{ck} \tag{17}$$

where all the parameters have the same meanings as it is described in DLT5085 (1999) code above.

The results gained from different codes are listed in Table 4. M_u is the average moment capacity value of a group of specimens, M_u^T is the calculated value. Referring to AIJ, BS5400, EC4, AISC-LRFD and DBJ13-15, the mean values for CS-165-2.5-30 group are 0.907, 0.817, 1.007, 1.352 and 1.041 which are larger and abnormal in compare with the other group's results. So, (CS-165-2.5-30) group is not included in Table 5 because it can't describe the real condition.

Table 5. Calculated Flexural Capacity Results

Specimen	M_u/ kN·m	AIJ $\frac{M_u^C}{M_u}$	AISC-LRFD $\frac{M_u^C}{M_u}$	EC4 $\frac{M_u^C}{M_u}$	DL/T5085 $\frac{M_u^C}{M_u}$	DBJ13-51 $\frac{M_u^C}{M_u}$	Method 1 $\frac{M_u^C}{M_u}$	Method 2 $\frac{M_u^C}{M_u}$
CS-114-2.5-30	11.75	0.790	0.711	0.846	1.101	0.873	1.046	0.997
CS-114-2.5-50	12.47	0.744	0.670	0.808	1.099	0.864	1.000	1.095
CS-114-3.8-30	15.23	0.833	0.749	0.863	1.118	0.929	1.077	0.888
CS-114-3.8-50	16.75	0.757	0.681	0.795	1.062	0.875	0.993	0.919
CS-165-3.8-30	37.55	0.723	0.650	0.775	1.014	0.807	0.958	0.928
CS-165-3.8-50	38.86	0.698	0.628	0.760	1.040	0.820	0.940	1.049
MEAN		0.757	0.682	0.808	1.072	0.861	1.002	0.979
STDEV		0.048	0.043	0.040	0.041	0.044	0.052	0.093

By comparing the mean values and standard deviations (STDEV) that listed in table5; it can be recognized; DL/T5085 code gave the best accuracy among the codes consulted in this paper which, gave conservative results and moment capacity with more than 10% deviation from the test results. The results calculated by AIJ and AICS-LRFD are obviously small with deviation ratios more than 24% and 30% respectively and that may attributed to AIJ and AICS-LRFD calculation methods which ignore concrete contribution. Besides, in AICS-LRFD an extra reduction coefficient for the steel tube capacity have been considered.

5. FLEXURAL CAPACITY CALCULATION METHOD

5.1 Method of Mechanical Equilibrium

The stress distribution of steel apparently influences the capacity of specimen. So, the strain of steel tube corresponding to moment capacity is listed in Table 6. In this test, the moment capacity took the value when the maximum steel fiber strain was 0.01. Because strain 1 in Figure 2 is the maximum steel fiber strain, all the strains in Table 6 took the values when strain 1 is 0.01.

Table 6. The longitudinal strains of steel tube corresponding to the moment capacity

Specimen	Strain 1 ($\times10^{-6}$)	Strain 2 ($\times10^{-6}$)	Strain 3 ($\times10^{-6}$)	Strain 4 ($\times10^{-6}$)	Strain 5 ($\times10^{-6}$)
CFST114-2.5-30-A	10000	2195	-8408	2884	
CFST114-2.5-30-B	10012	2987	-7927	2650	
CFST114-2.5-30-C	10003	1806	-7350	2940	
CFST114-2.5-50-A	10029	2669	-8284	1909	
CFST114-2.5-50-B	10051	2791	-3790	2689	
CFST114-2.5-50-C	9994	3163	-8256	2445	
CFST114-3.8-30-A	10034	1381	-7373	2130	
CFST114-3.8-30-B	10024	2445	-7408	-	
CFST114-3.8-30-C	10001	1517	-7416	2423	
CFST114-3.8-50-A	10033	2793	-9585	2479	
CFST114-3.8-50-B	9966	1216	-8032	1603	
CFST114-3.8-50-C	10107	464	-8683	1361	
CFST165-2.5-30-A	10010	7144	3043	-5542	-5976
CFST165-2.5-30-B	10093	9238	4193	-1962	-3886

CFST165-2.5-30-C	9995	7626	2342	-1326	-3040
CFST165-3.8-30-A	10031	7065	2528	-3475	-5494
CFST165-3.8-30-B	10056	6194	2526	-3429	-4309
CFST165-3.8-30-C	10061	7442	2846	-2663	-4246
CFST165-3.8-50-A	9981	9047	1805	-1715	-5824
CFST165-3.8-50-B	10003	7869	3528	-5346	-4892
CFST165-3.8-50-C	10000	7600	2849	-1814	-3685

Referring to table 6, almost all the strain values are larger than 2000×10^{-6} in response to the beam moment capacity. As the yield strain of steel in this test is about 2000×10^{-6}; the whole steel section yielded corresponding to the moment capacity. If the strain of concrete assumed to reach to the concrete strength corresponding to the moment capacity, then stress distribution and calculation chart may describe as it can be seen in Figure 12.

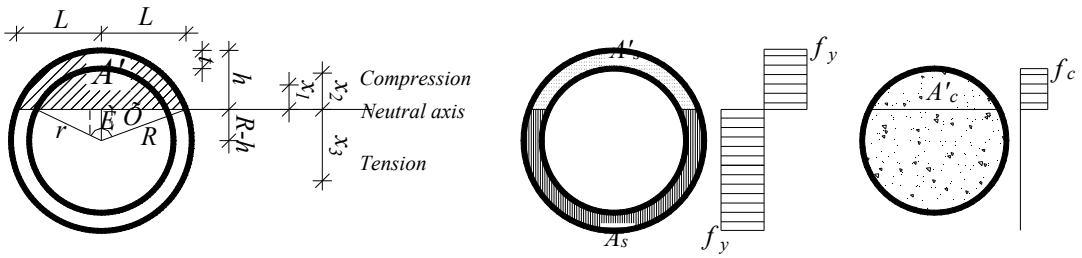

(a) Whole section (b) Steel tube (c) Concrete

Figure 12. Cross-Sectional Stress Distribution Corresponding to Moment Capacity

Due to the concrete weakness in tension its impact in the tension zone was ignored. Based on the mechanical equilibrium on the whole section, an equilibrium equation can be expressed in Eq. 18.

$$A_s f_y = A_c' f_c + A_s' f_y' \tag{18}$$

where, A_s is the tension area of steel; A_s' is the compression area of steel; A_c' is the compression area of concrete; $f_y' = f_y$ is the compressive strength of steel; f_c is the constrained concrete strength. All the area can be calculated with the size of the section.

From the previous study carried [23], the strength of constrained concrete of steel may calculated by expression (19).

$$f_c = f_{ck} + k \bullet p \tag{19}$$

where, k is an enhancing coefficient and according to this study result for LACFST can take a value equal to 3.4 and P is the confining force.

$$p = 2t\sigma_{sh} / D = 2t\upsilon\sigma_l / D \tag{20}$$

where, σ_{sh} is the circumferential stress; σ_l is the longitudinal stress; υ is the lateral deformation coefficient. When reaching to the beam moment capacity, $\sigma_l = f_y$ and υ can take the Poisson's ratio of steel. So, the following expression can be got.

$$f_c = f_{ck} + 2k\upsilon f_y / D \tag{21}$$

After calculating the height of the compression area (h) the moment capacity of the section can be found from expression (22).

$$M_u = A_c' f_c x_1 + A_s' f_y' x_2 + A_s f_y x_3 \tag{22}$$

where, x_1, x_2 and x_3 are the distances between the centroid of compression concrete, compression steel and tension steel area to the neutral axis respectively.

5.2 Method of Combined Strength

The method of mechanical equilibrium seems complex. So, an attempt to find a simple method similar to that one proposed by Han Linhai [6] was carried out. Accordingly; the moment capacity M_u can be calculated by using expression (23).

$$M_u = \gamma_m W_{sc} f_{sc} \tag{23}$$

$$f_{sc} = N_u / A_{sc} \tag{24}$$

where, γ_m is an enhancement coefficient considering the contribution of steel after yielded; N_u is the compressive capacity of a stub LACFST specimen. If the concrete increment strength Considered; N_u can be following expressed according to previous study [24].

$$N_u = f_y A_s + \beta f_{ck} A_c \tag{25}$$

Where β is the concrete strength increment coefficient and expressed by the following form according to previous study [24]:

$$\beta = 1.36 + 0.3\ \xi \tag{26}$$

Therefore, the capacity of LACFST short stub may calculate by expression (17), and can simplify as shown in Eq. 28. The two expressions (27) and (28) have showed good accuracy to calculate the bearing capacity. The results of expression (27) had a mean of 1.011 with STDEV of 0.045, while the results of expression of (28) had a mean of 0.997 with STDEV of 0.045[24] hence, they are reliable to use.

$$N_u = 1.3 f_y A_s + 1.36 f_{ck} A_c \tag{27}$$

$$N_u = 1.35(f_y A_s + f_{ck} A_c) \tag{28}$$

So, the two Eqs 29 and 30 can be used to calculate the strength of LACFST and the moment capacity respectively. Steel tube yielded when the section reached to its moment capacity, thus, the enhancement coefficient γ_m can take a value of 1.1.

$$f_{sc} = \frac{N_u}{A_{sc}} = \frac{1.35(f_y A_s + f_{ck} A_c)}{A_s + A_c} = \frac{1.35(1+\xi) f_{ck} A_c}{A_s + A_c} \tag{29}$$

$$M_u = 0.17 \gamma_m D(1+\xi) f_{ck} A_c \tag{30}$$

5.3 Comparison of the Results

Table 5 shows the results of the two methods used in this paper to calculate the moment capacity. Besides, Figure 13 was drawn to compare the calculated results and the test ones (Method 1 and Method 2 referred to the method of mechanical equilibrium and the method of combined strength respectively). From the figure, it can be seen that method 1 and method 2 has a mean of 1.002 and 0.979 with STDEV of 0.052 and 0.081 respectively where these figures reflect the good accuracy of the two methods. Because of the simplicity of method 2; the relation between the concrete strength increment coefficient and the confinement coefficient (ξ) expressed linearly. But it is proposed that this linear relation subject to further studies to get a more reliable expression. As a result of this comparison it is suggested to use method 1 to calculate the moment capacity.

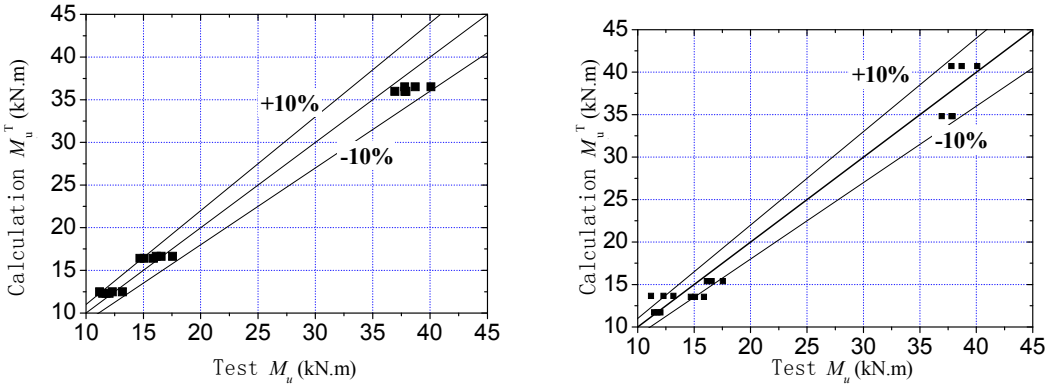

(a)Method 1 (b) Method 2

Figure 13. Comparison of Calculation and Test Results

6. NUMERICAL ANALYSIS

6.1 Constitutive Model of LAC

Formula of $\varepsilon_c = 1788 + 17.58 f_c$ was proposed to calculation the strain peak value of LAC without constraint [25]. It was used to establish the numerical mode of confined concrete in compressive region. Based on the model of confined normal concrete by Han Linhai [26], the model of confined LAC was proposed. In the model of this paper, the boundary value of confinement coefficient ξ was higher than the one in the model of confined normal concrete. This is because the enhanced strength by the restrain of steel tube for LAC is lower than the one of normal concrete. The relationship between strain and material strength was also fitted based on the previous experimental results [23].

The model of confined LAC in compressive region was proposed as following.

$$\sigma = \begin{cases} \sigma_o[A\dfrac{\varepsilon}{\varepsilon_o} - B(\dfrac{\varepsilon}{\varepsilon_o})^2] & (\varepsilon \le \varepsilon_o) \\ \sigma_0(1-q) + \sigma_0 q(\dfrac{\varepsilon}{\varepsilon_0})^{0.1\xi} & (\varepsilon > \varepsilon_o, \xi \ge 1.22) \\ \sigma_0(\dfrac{\varepsilon}{\varepsilon_0})\dfrac{1}{\beta(\varepsilon/\varepsilon_0 - 1)^2 + \varepsilon/\varepsilon_0} & (\varepsilon > \varepsilon_o, \xi < 1.22) \end{cases} \quad (31)$$

where, $\sigma_o = f_{ck}[1.194 + (\frac{13}{f_{ck}})^{0.45}(-0.07485\xi^2 + 0.5789\xi)]$

$$\varepsilon_o = \varepsilon_c + [1000 + 800(\frac{f_{ck} - 24}{24})]\xi^{0.2}$$

$$\varepsilon_c = 1788 + 17.58 f_{ck}$$

$$A = 2.0 - k$$

$$B = 1.0 - k$$

$$k = 0.1\xi^{0.745}$$

$$q = \frac{k}{0.2 + 0.1\xi}$$

$$\beta = (2.36 \times 10^{-5})^{[0.25 + (\xi - 0.5)^7]} \times 5.0 \times f_{ck}^2 \times 10^{-4}$$

The above model was used to calculate the relationship between stress and strain for confined LAC. In Figure 14, the calculation result was compared to the previous experimental one. The detailed introduction about the experiment can be found in reference [23]. In the figure, the specimens were the same one in reference [23]. The load acted on the steel was eliminated and the experiment curves of concrete were gained. From the figures, it shows that the model calculation results were identical with the experiment ones as well. So, the proposed model for confined LAC in this paper was reasonable and can be used in the analysis.

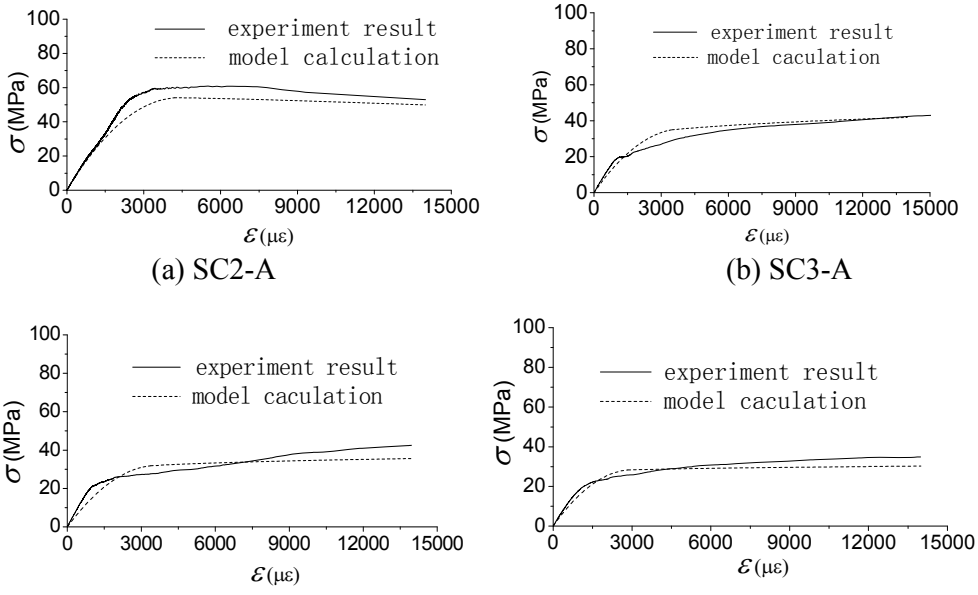

(a) SC2-A (b) SC3-A

(c) SC4-A (d) SC5-A

Figure 14. Comparison of Confined LAC Model and Experiment Result

The model of confined LAC in tensile region used the model proposed by Han Linhai [26] as following.

$$\sigma_c = \begin{cases} \sigma_p[1.2\varepsilon_c / \varepsilon_p - 0.2(\varepsilon_c / \varepsilon_p)^6] & \varepsilon_c \le \varepsilon_p \\ \sigma_p \dfrac{\varepsilon_c / \varepsilon_p}{0.31\sigma_p^2(\varepsilon_c / \varepsilon_p - 1)^{1.7} + \varepsilon_c / \varepsilon_p} & \varepsilon_c > \varepsilon_p \end{cases} \quad (32)$$

where, σ_p is the peak value of stress, it can be calculated as $\sigma_p = 0.26(1.25 f_{ck})^{2/3}$. ε_p is the strain corresponding to the peak value of stress, it can be calculated as $\varepsilon_p = 43.1\sigma_p \times 10^{-6}$.

6.2 The analysis model and result

In order to make FEM model, following assumptions were adopted. (1) The deformation of specimen's section agrees with the Bernoulli-Euler's theory at various loading stages. (2) There was no slip between the steel tube and LAC. (3) The deflection along the length distributed as half sine wave. All of the above three assumptions were proved by the experimental results.

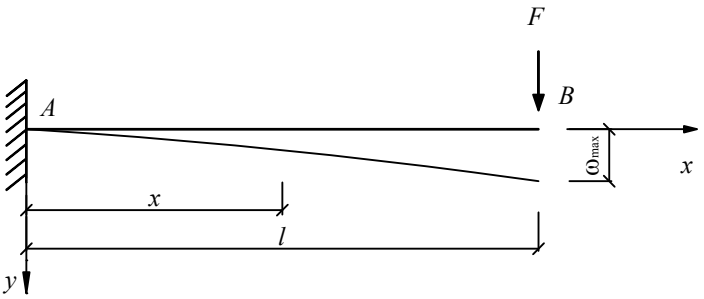

Figure 15. The Simplified Calculation Model for Flexural Behavior of LACFST

The calculation model was simplified to be a cantilever beam model which could reflect the same behavior of the test process. The simplified calculation model is shown in Figure 15. In ANSYS program, SOLID65 was used for LAC and SOLID186 was used for steel tube. Element of TARGE170 and CONTA173 were used for the contact relationship between steel tube and LAC. The mechanical properties of LAC and steel were the same to the results from the test. Von Mises kinematic hardening rule was adopted for steel material. In the stage of plastic hardening, the tangent modulus of steel took $0.01E_s$ (E_s is Elastic modulus of steel). In this analysis, the displacement loading method was used.

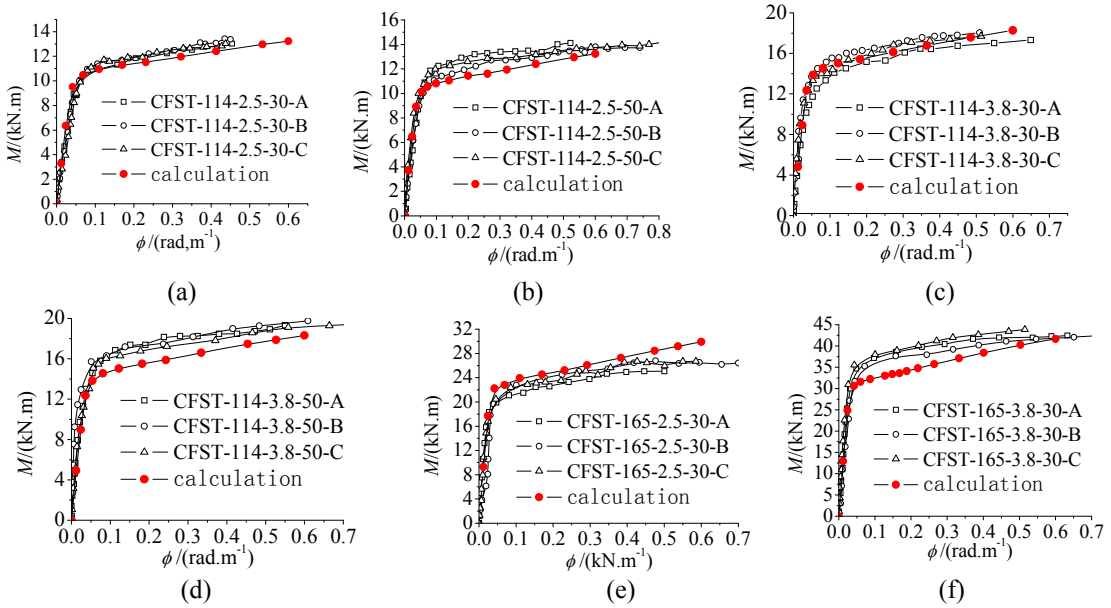

Figure 16. Comparison of Test and Calculation Results

The calculation results are shown in Figure 16. As the figure shows, the calculation results fit with the experiment results well. So, it can be got that the constitutive model of LAC established in this paper can be used for the analysis of LACFST with good accuracy.

7. CONCLUSIONS

(1) From the test noticed the strain distribution and the deflection distribution along the length at various loading stages agrees with the Bernoulli-Euler's theory and half sine wave curve respectively.

(2) Filling with LAC can obviously improve the flexural behavior of steel tube. The moment capacity of LACFST increased as the steel ratio and LAC concrete strength increased. The shear span ratio almost has no influence on the flexural behavior of LACFST. The increment of moment capacity was not obvious when the high strength LAC used.

(3) Compared to other codes mentioned in this paper, the method of AIJ (1997) has a good accuracy for calculation the stiffness. And the results using DL/T5085 to calculate moment capacity are closest to the test ones with a mean of 1.072 and STDEV of 0.041. Besides, the deviation of moment capacity calculation using other codes is 10% more or less than the test one.

(4) Two methods were provided in this paper; the method of mechanical equilibrium and the method of combined strength which has a mean of 1.002 and 0.979 with STDEV of 0.052 and 0.081 respectively. Therefore, from this study it is possible to suggest that both methods can be used to calculate the moment capacity.

(5) The constitutive model of confined LAC in compressive region was established. And it was proved to be accuracy enough. Based on some assumptions which were proved reasonable by the test, the constitutive model was used in the FEM to analyze the flexural behavior and the results fit with the experiment results well.

ACKNOWLEDGMENTS

The authors appreciate the support of The National Natural Science Fund (No.51208176); The authors appreciate the support of China Postdoctoral Science Foundation (2012M511187), The Fundamental Research Funds for the Central Universities (2012B02914).

REFERENCES

[1] Ge, H.B., Susantha, K.A.S., Satake, Y., et al., "Seismic Demand Predictions of Cconcrete-filled Steel Box Columns", Engineering Structures, 2003,Vol. 25, No. 3, pp. 337-345.

[2] Gao, S.B. and Ge, H.B., "Numerical Simulation of Hollow and Concrete-filled Steel Columns", Advanced Steel Construction, 2007, Vol. 3, No. 3, pp. 668-678.

[3] Montejo, L.A., Gonzalez-Roman, L.A. and Kowalsky, M.J., "Seismic Performance Evaluation of Reinforced Concrete-Filled Steel Tube Pile/Column Bridge Bents", Journal of Earthquake Engineering, 2012, Vol. 16, No. 3, pp. 401-424.

[4] Morcous, G., Hanna, K., Deng, Y., et al., "Concrete-Filled Steel Tubular Tied Arch Bridge System: Application to Columbus Viaduct ", Journal of Bridge Engineering, 2012, Vol. 17, No. 1, pp. 107-116.
[5] Kang, J.Y., Choi, E.S., Chin, W.J., et al, "Flexural Behavior of Concrete-filled Steel Tube Members and its Application", International Journal of Steel Structures, 2007, Vol. 7, No. 4, pp.319-324.
[6] Mossahebi, N., Yakel, A. and Azizinamini, A., "Experimental Investigation of a Bridge Girder made of Steel Tube Filled with Concrete", Journal of Constructional Steel Research, 2005, Vol. 61, No. 3, pp. 371-386.
[7] Mohamed, H.M. and Masmoudi, R., "Flexural Strength and Behavior of Steel and FRP-reinforced Concrete-filled FRP Tube Beams", Engineering Structures, 2010, Vol. 32, No. 11, pp. 3789-3800.
[8] Soundararajan, A. and Shanmugasundaram, K., "Flexural Behaviour of Concrete-Filled Steel Hollow Sections Beams", Journal of Civil Engineering and Management, 2008, Vol.14, No. 2, pp. 107-114.
[9] Han, LH, "Flexural Behaviour of Concrete-filled Steel Tubes", Journal of Constructional Steel Research, 2004, Vol. 60, No. 2, pp. 313-337.
[10] Deng, Y., Tuan, C.Y. and Xiao, Y., "Flexural Behavior of Concrete-Filled Circular Steel Tubes under High-Strain Rate Impact Loading", Journal of Structural Engineering-ASCE, 2012, Vol. 138, No. 3, pp. 449-456.
[11] Nakamura, S., Momiyama, Y., Hosaka, T., et al., "New Technologies of Steel/Concrete Composite Bridges", Journal of Constructional Steel Research, 2002, Vol. 58, No. 1, pp. 99-130.
[12] Ghannam, S, Jawad, Y.A. and Hunaiti, Y., "Failure of Lightweight Aggregate Concrete-Filled Steel tTubular Columns", Steel and Composite Structures, 2004, Vol. 4, No. 1, pp. 1-8.
[13] Mouli, M. and Khelafi, H., "Strength of Short Composite Rectangular Hollow Section Columns Filled with Lightweight Aggregate Concrete", Engineering Structures, 2007, Vol. 29, No. 8, pp. 1791-1797.
[14] Assi, I.M., Qudeimat, E.M. and Hunaiti, Y., "Ultimate Moment Capacity of Foamed and Lightweight Aggregate Concrete-filled Steel Tubes", Steel and Composite Structures, 2003, Vol. 3, No. 3, pp. 199-212.
[15] Fu, Z.Q., Ji B.H, Lv, L. and Zhou, W.J., "The Behavior of Lightweight Aggregate Concrete Filled Steel Tube Slender Columns under Axial Compression", Advanced Steel Construction, 2011, Vol. 7, No. 2, pp. 144-156.
[16] Elzien, A., Ji, B.H., Fu, Z.Q. and Hu, Z.Q, "The Behavior of Lightweight Aggregate Concrete Filled Steel Tube Columns under Eccentric Loading", Steel and Composite Structures, 2011, Vol. 11, No. 6, pp. 469-488.
[17] Architectural Institute of Japan (AIJ), "Recommendations for Design and Construction of Concrete Filled Steel Tubular Structures", 1997.
[18] British Standard Institute, "BS5400, Part 5, Concrete and Composite Bridges", 1979.
[19] Eurocode 4, "Design of Composite Steel and Concrete Structures", 1994.
[20] AISC, "Load and Resistance Factor Design Specification for Structural Steel Buildings", 1999.
[21] Engineering Construction Standard of Fujian Province of China, "Technical Specification for Concrete-Filled Steel Tubular Structures", 2003. (In Chinese)
[22] Electric Power Industry Standard of China, "Code for Design of Steel-Concrete Composite Structures", 1999. (In Chinese)
[23] Fu, Z.Q., Ji B.H., Lv, L. and Yang M., "The Mechanical Properties of Lightweight Aggregate Concrete Constrained by Steel Tube", Geotechnical Special Publication ASCE, 2011, No. 219, pp. 33-39.

[24] Fu, Z.Q., Ji B.H., Zhou, Y. and Wang X.L., "An Experimental Behavior of Lightweight Aggregate Concrete Filled Steel Tubular Stub under Axial Compression", Geotechnical Special Publication ASCE, 2011, No. 219, pp. 24-32.
[25] Wang, P. T., Shah, S. P. and Naaman, A.E., "Stress-Strain Curves of Normal and Lightweight Concrete in Compression", Journal of American Concrete Institute, 1978, Vol. 75, No. 11, pp. 603-611.
[26] Han, L.H., "Concrete Filled Steel Tube Structure - Theory and Application (Second Edition)", Science Press, 2007. (In Chinese)